Electronic Supplementary Material (ESI) for Nanoscale.

Electronic Supplementary Information

Silver-mediated temperature-controlled selective deposition of Pt on hexoctahedral Au nanoparticles and the high performance of Au@AgPt NPs on catalysis and SERS

*Chunyuan Song, Youzhi Sun, Jinxiang Li, Chen Dong, Jingjing Zhang, Xinyu Jiang, Lianhui Wang**

Key Laboratory for Organic Electronics and Information Displays & Jiangsu Key Laboratory for Biosensors, Institute of Advanced Materials (IAM), Jiangsu National Synergetic Innovation Center for Advanced Materials (SICAM), Nanjing University of Posts & Telecommunications, Nanjing 210023, China.

∗Corresponding author.

E-mail addresses: iamlhwang@njupt.edu.cn

EXPERIMENT SECTION

Materials. Gold(III) chloride trihydrate ($HAuCl_4·3H_2O$, ≥49.87% Au), (1-hexadecyl) trimethylammonium chloride (CTAC, 96%), and sodium borohydride ($NaBH_4$, 98%) were purchased from Alfa Aesar. Chloroplatinicacid hexahydrate ($H_2PtCl_6·6H_2O$, ≥37.5% Pt), ascorbic acid (AA, 99.7%), and silver nitrate ($AgNO_3$, 99.8%) were provided by Sinopharm Chemical Reagent Co., Ltd. 4-Nitrothiophenol (4-NTP, 80%) was obtained from Sigma-Aldrich. Methylene blue (MB, 90%) was bought from Macklin. All the aforementioned materials were used as received and the aqueous solutions were prepared with ultrapure water (Milli-Q Direct 8, Millipore, France) with a resistivity of 18.2 MΩ·cm.

Synthesis of Hexoctahedral Au Nanoparticles. Hexoctahedral Au nanoparticles (Au HNPs) were synthesized by a facile, one-pot, seedless synthesis by using AA to reduce $HAuCl_4$ in the presence of CTAC as surfactant. Specifically, 1 mL of 10 mM $HAuCl_4$ aqueous solution was mixed with 10 mL of 200 mM CTAC aqueous solution, followed by quickly adding 500 μL of 300 mM AA. The mixture was stirred vigorously for 2 min at room temperature and then transferred into a 35°C thermotank and maintained undisturbedly for 3 h. The product was then purified by three times centrifugations (1000 rpm for 10 min) and finally re-dispersed in 10 mL water for further usage.

Synthesis of Au@AgPt Nanoparticles. The standard method for synthesizing Au@AgPt NPs is as follows. Briefly, 1 mL Au HNPs were diluted into 3.5 mL water, followed by adding 500 μL of 200 mM aqueous CTAC and 10 μL of 2 mM aqueous $AgNO_3$ in sequence under violent stirring. After that, 40 μL of 100 mM AA was added and the mixture was gently stirred for 1.5 h in a thermotank to coat Ag shells on the Au HNPs. To deposit Pt on Au@Ag NPs, 60 μL of 10 mM H_2PtCl_6 aqueous solution was added into the mixture under gentle stirring and the Pt atoms were allowed to deposit onto the Au HNPs for 2 h in the thermotank. The product was centrifugally purified (1500 rpm for 5 min), and the precipitates were re-dispersed in 1 mL water to obtain the final Au@AgPt NPs. Herein, four types of Au@AgPt NPs (named 20-Au@AgPt NPs, 25-Au@AgPt NPs, 35-Au@AgPt NPs and 50-Au@AgPt NPs) were fabricated by controlling the growth temperatures (i.e. temperatures of thermotank) at 20°C, 25°C, 35°C, and 50°C, respectively. For investigating the influence of Pt precursor on the selective deposition of Pt on Au HNPs, the volume of H_2PtCl_6 aqueous solution was adjusted and the other parameters were fixed.

SERS Characterizations. For characterizing the SERS properties of the nanoparticles, each SERS sample was prepared by mixing 10 μL of 1 mM 4-NTP with 100 μL of the nanoparticles under vigorous shaking. After 3 hours, 20 μL mixture was dropped into a PDMS molded well (4 mm diameter, 1 mm height) on a clean silicon wafer, followed by SERS scans the natural dried sample at different spots with the parameters setting as 785 nm laser, 0.1% power, 1 s exposure time, 20 × objective lens. For each sample, ten scans were recorded at different positions and the baselines of the spectra were removed by the software Wire 4.0. Finally, an averaged SERS spectrum of each sample was obtained. For normal Raman detection, 10 μL of 100 mM 4-NTP was pipetted into a PDMS molded well (4 mm diameter, 1 mm height) on a clean silicon wafer and the Raman measurement were performed as same as the SERS.

The SERS enhancement factor (EF) was calculated using the following equation:

$$EF = \frac{I_{\mathrm{SERS}}}{I_{\mathrm{normal}}} \frac{N_{\mathrm{normal}}}{N_{\mathrm{SERS}}}$$

Where I_{SERS} and I_{normal} denote the peak (1335 cm^{-1}) intensity of the SERS and normal Raman signals, respectively; N_{SERS} and N_{normal} represent the amount of Raman molecules contributing the signal, respectively. It is assumed that in the case of SERS and Normal, the 4-NTP modified nanoparticles (SERS) and molecules (Normal) are uniformly distributed on the surface of the silicon wafer. Thus, the surface density of molecular distributions of 4-NTP, i.e. σ_{SERS} and σ_{Normal}, can be calculated according to the total added molecules and the area of the well, respectively. Since the same objective lens is used to scan SERS and normal Raman, the spot diameter of the laser beam is same. Therefore, the $N_{\text{normal}}/N_{\text{SERS}}$ is equivalent to $\sigma_{\text{normal}}/\sigma_{\text{SERS}}$.

Catalytic Activity Characterizations. To study the catalytic properties of the as-prepared Au@AgPt NPs, chemical reduction of MB by reducing agent $NaBH_4$ in the presence of catalyst Au@AgPt NPs was taken as a reaction model. Specifically, 3.5 mL of 0.05 mM MB solution was added into a cuvette, followed by adding 140 μL Au@AgPt NPs and 350 μL of 500 mM $NaBH_4$ in sequence. Then the cuvette was sealed off immediately by covering with a compact lid. After that, the time-dependent absorption spectra were recorded at once by a Shimadzu UV-3600 UV-vis-NIR spectrophotometer.

In Situ SERS Monitoring of Catalytic Reaction. The in situ SERS monitoring of catalytic reaction of 4-NTP was carried out as follows. Firstly, 20 μL of 35-Au@AgPt NPs (0.4 mg/mL) was mixed with 2 μL of 1 mM 4-NTP solution in a well on a Si wafer. After natural air drying, 20 μL of 2 mM $NaBH_4$ solution was added into the Au@AgPt NPs seeded well, followed by immediate SERS measurements (785 nm laser beam, 10 mW power, 50× long working distance objective, acquisition time 10 s), and the SERS signals were collected every minute to obtain a dynamic monitoring of the catalytic reaction. For SERS monitoring of the catalytic reaction of MB, 10 μL of 35-Au@AgPt NPs was dropped in a well on a Si wafer and left to dry naturally.

Then, 20 μL of 0.05 mM MB was added into the well, and 2 μL of 10 mM $NaBH_4$ was added in sequence, followed by immediately SERS measurements of time series test mode with 1 s interval. The parameters of the SERS test were set to 785 nm laser beam, 100 mW power, 50× long working distance objective, and acquisition time 1 s.

Instruments. Absorption spectra were collected by a Shimadzu UV-3600 UV-vis-NIR spectrophotometer. A Hitachi S-4800 scanning electron microscopy (SEM) equipping with an Oxford INCA-350 energy dispersive X-ray microanalysis system was used to record SEM images and perform energy dispersive spectrometry (EDS) analysis. A Hitachi HT7700 transmission electron microscopy (TEM) with 100 kV acceleration voltage was used to take TEM images. The HAADF-STEM-EDS characterizations were performed on a JEOL JEM-2100F high-resolution transmission electron microscopy (HRTEM) with 200 kV acceleration voltage. The selected area electron diffraction (SAED) was performed on a FEI Tecnai G2 TEM. The element content in the sample was also measured by a Perkin-Elmer Elan DRCII inductively coupled plasma mass spectrometry (ICP-MS). A CARON 6040-3 thermotank with high temperature resolution ± 0.1°C was used to provide controllable temperature from 5-70°C. The SERS spectra were recorded by a Renishaw InVia confocal Raman microscope equipping with a 785 nm laser.

RESULTS:

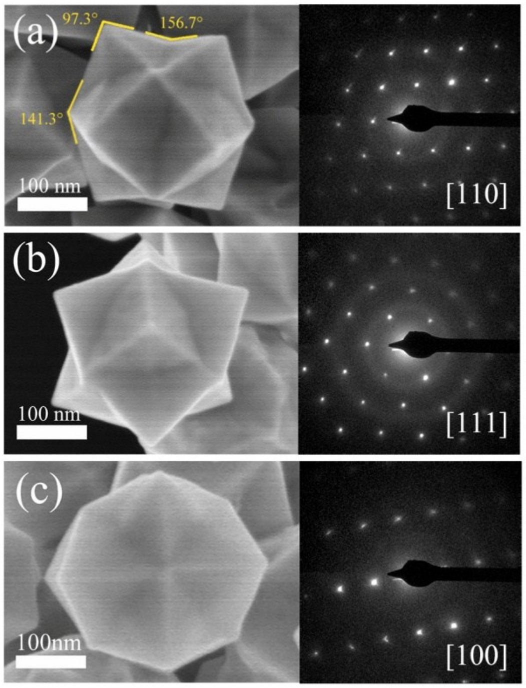

Figure S1. SEM images and corresponding SAED patterns of the Au HNPs viewed along the (a) [110], (b) [111] and (c) [100] directions.

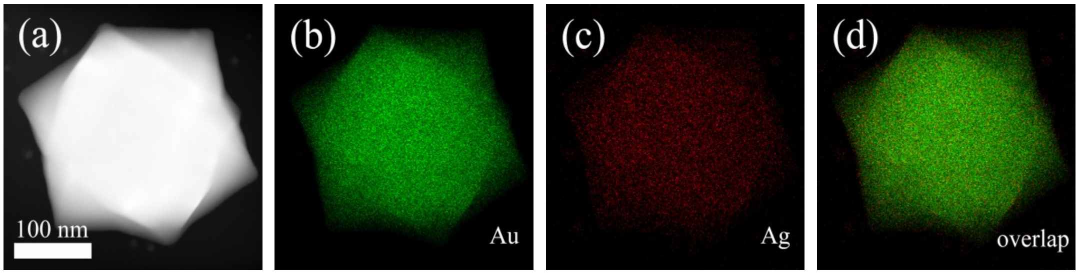

Figure S2. (a) HAADF-STEM image of Au@Ag NP. EDS maps of the (b) Au and (c) Ag distributions in the Au@Ag NP from (a). (d) The overlapped image of Au and Ag elements.

Table S1. Element content of Ag and Au in Au@Ag NPs

Elements	Weight ratio (wt%)	Atomic ratio (at%)
Ag	1.17	2.11
Au	98.83	97.89

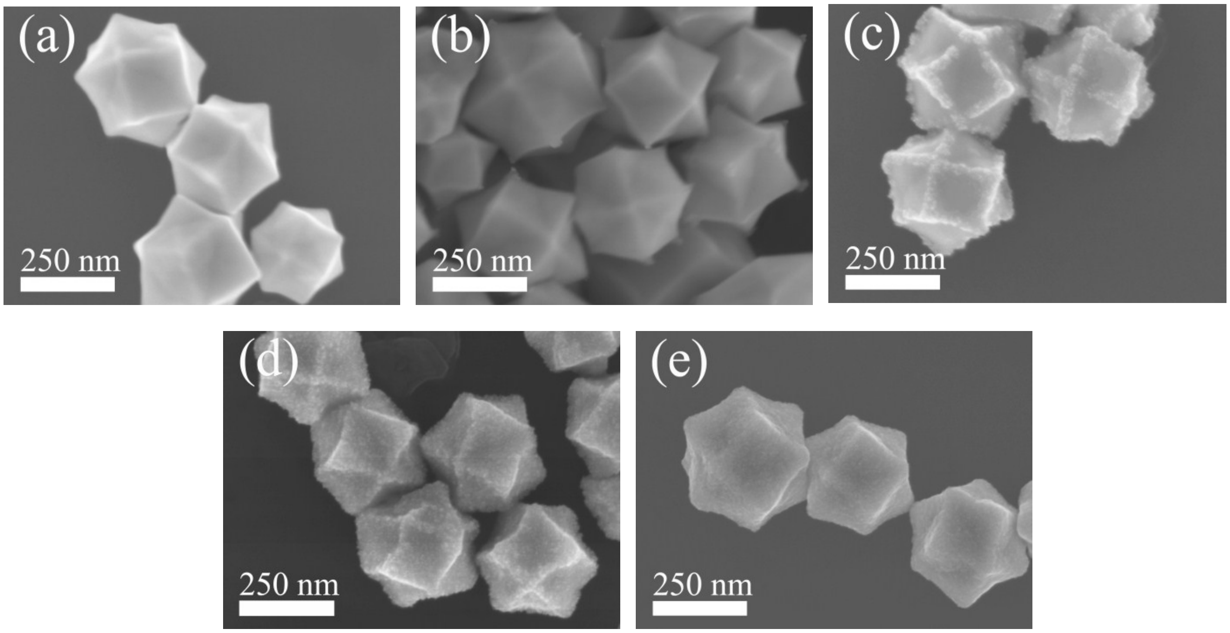

Figure S3. SEM images of Au HNPs (a), 20-Au@AgPt NPs (b), 25-Au@AgPt NPs (c), 35-Au@AgPt NPs (d) and 50-Au@AgPt NPs (e).

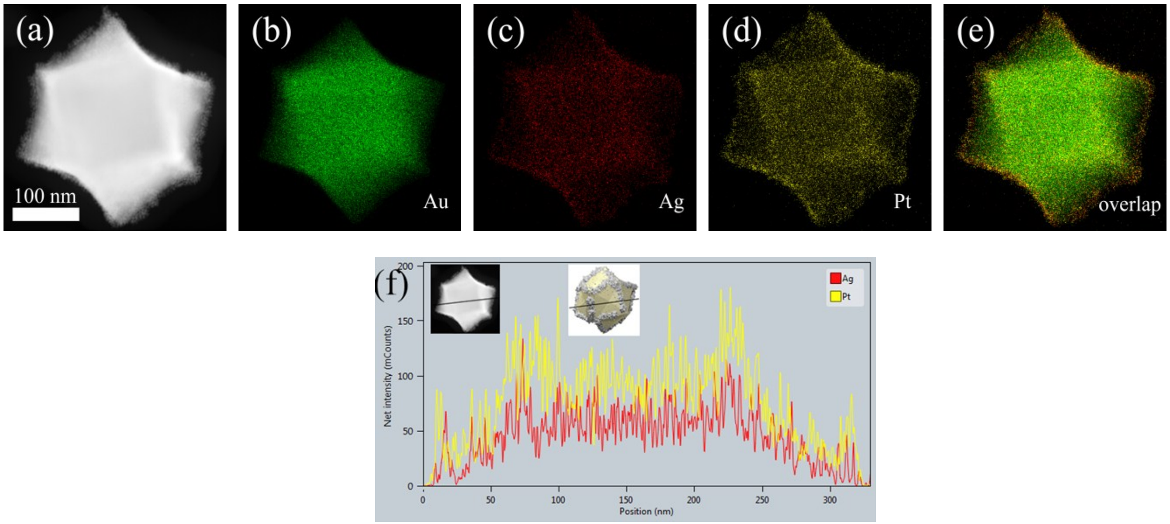

Figure S4. (a) HAADF-STEM image of the 25-Au@AgPt NP. EDS maps of the (b) Au, (c) Ag and (d) Pt distributions in the Au@AgPt NP from (a). (e) The overlapped image of Au, Ag and Pt elements. (f) EDS line-scan profile of Au@AgPt NP in which the red line represents the amount of Ag atoms, and the yellow line represents the amount of Pt atoms.

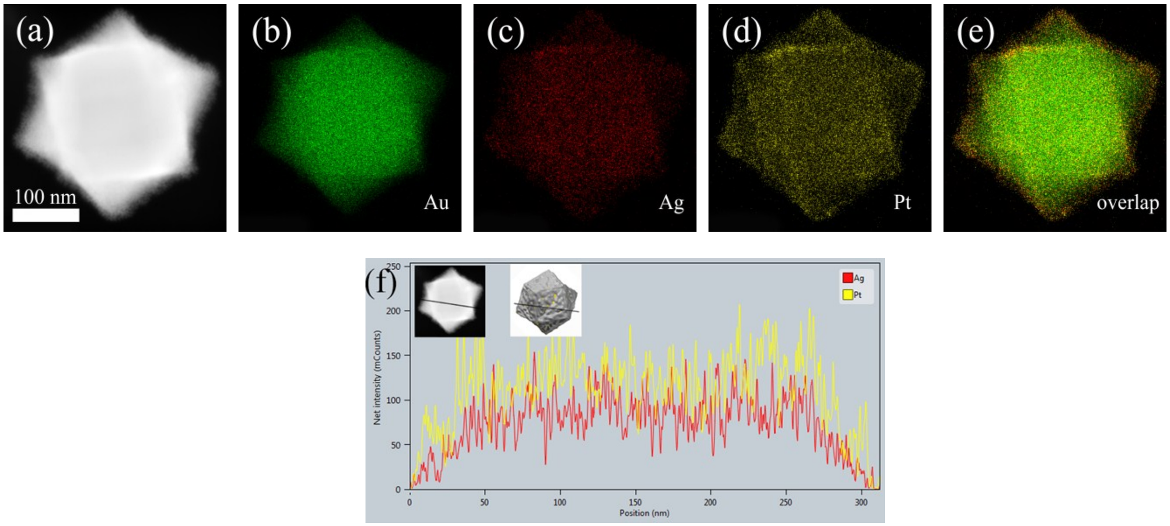

Figure S5. (a) HAADF-STEM image of the 35-Au@AgPt NP. EDS maps of the (b) Au, (c) Ag and (d) Pt distributions in the Au@AgPt NP from (a). (e) The overlapped image of Au, Ag and Pt elements. (f) EDS line-scan profile of Au@AgPt NP in which the red line represents the amount of Ag atoms, and the yellow line represents the amount of Pt atoms.

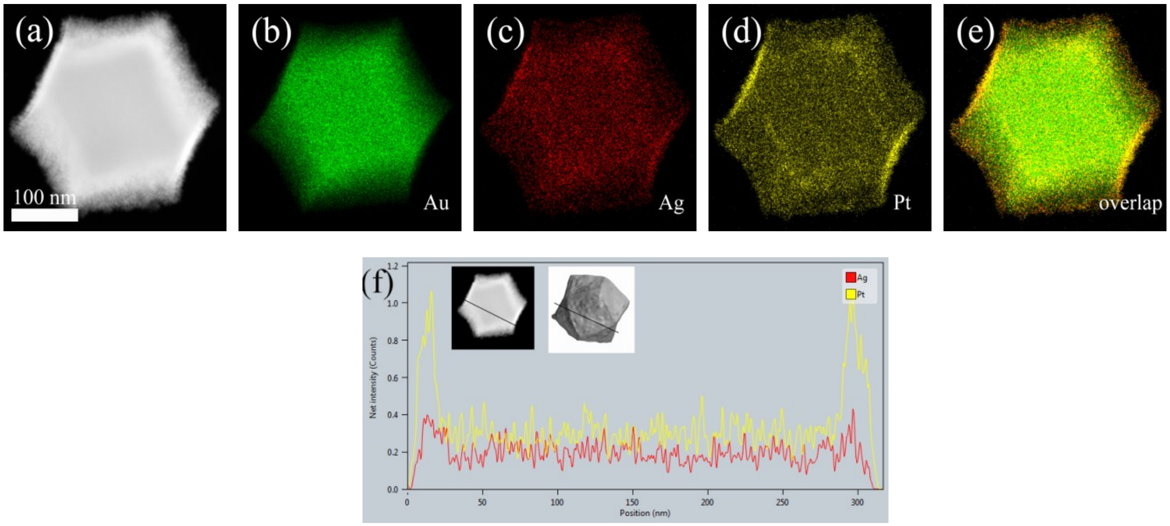

Figure S6. (a) HAADF-STEM image of the 50-Au@AgPt NP. EDS maps of the (b) Au, (c) Ag and (d) Pt distributions in the Au@AgPt NP from (a). (e) The overlapped image of Au, Ag and Pt elements. (f) EDS line-scan profile of Au@AgPt NP in which the red line represents the amount of Ag atoms, and the yellow line represents the amount of Pt atoms.

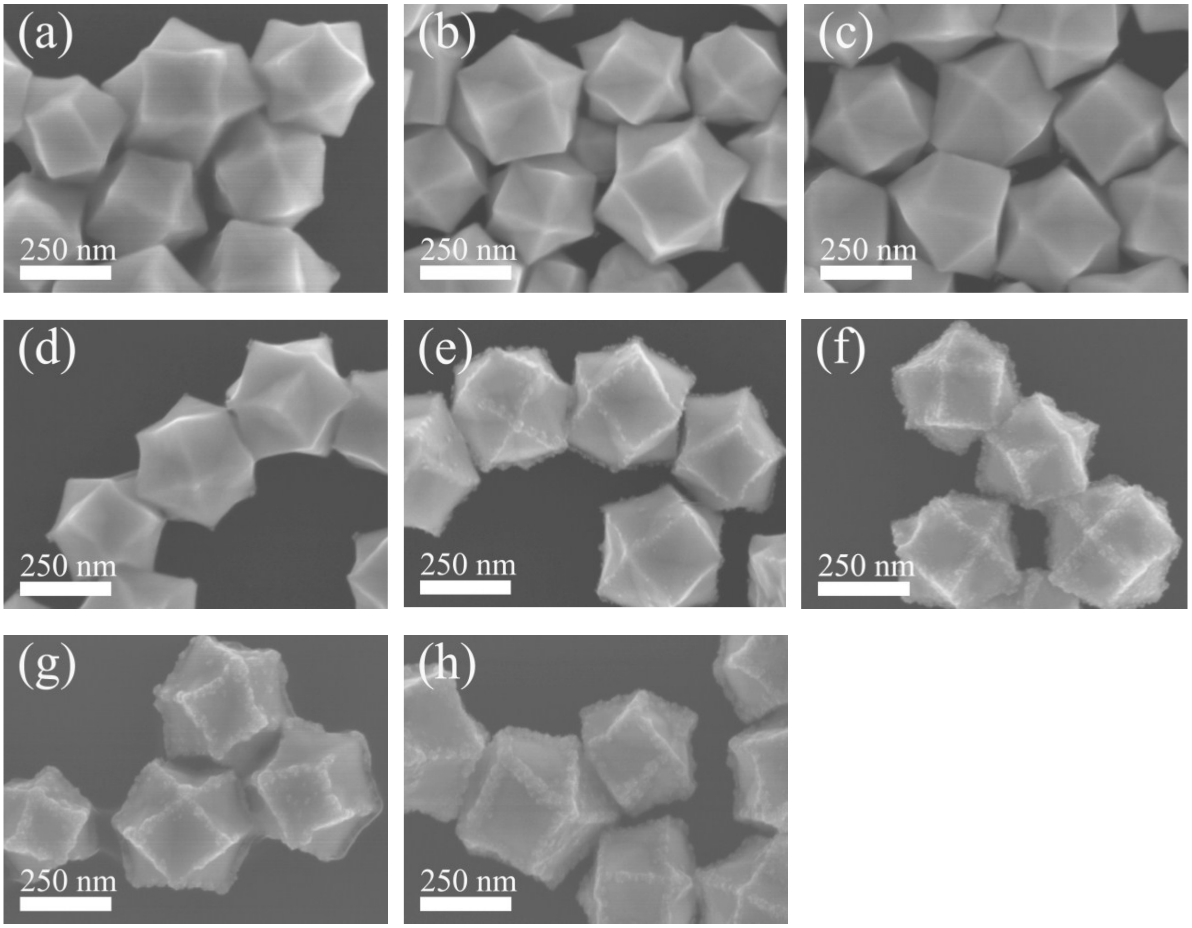

Figure S7. (a) SEM image of Au HNPs. (b)-(h) SEM images of 25-Au@AgPt NPs synthesized for different growth times 10, 20, 40, 60, 80, 100 and 120 min, respectively.

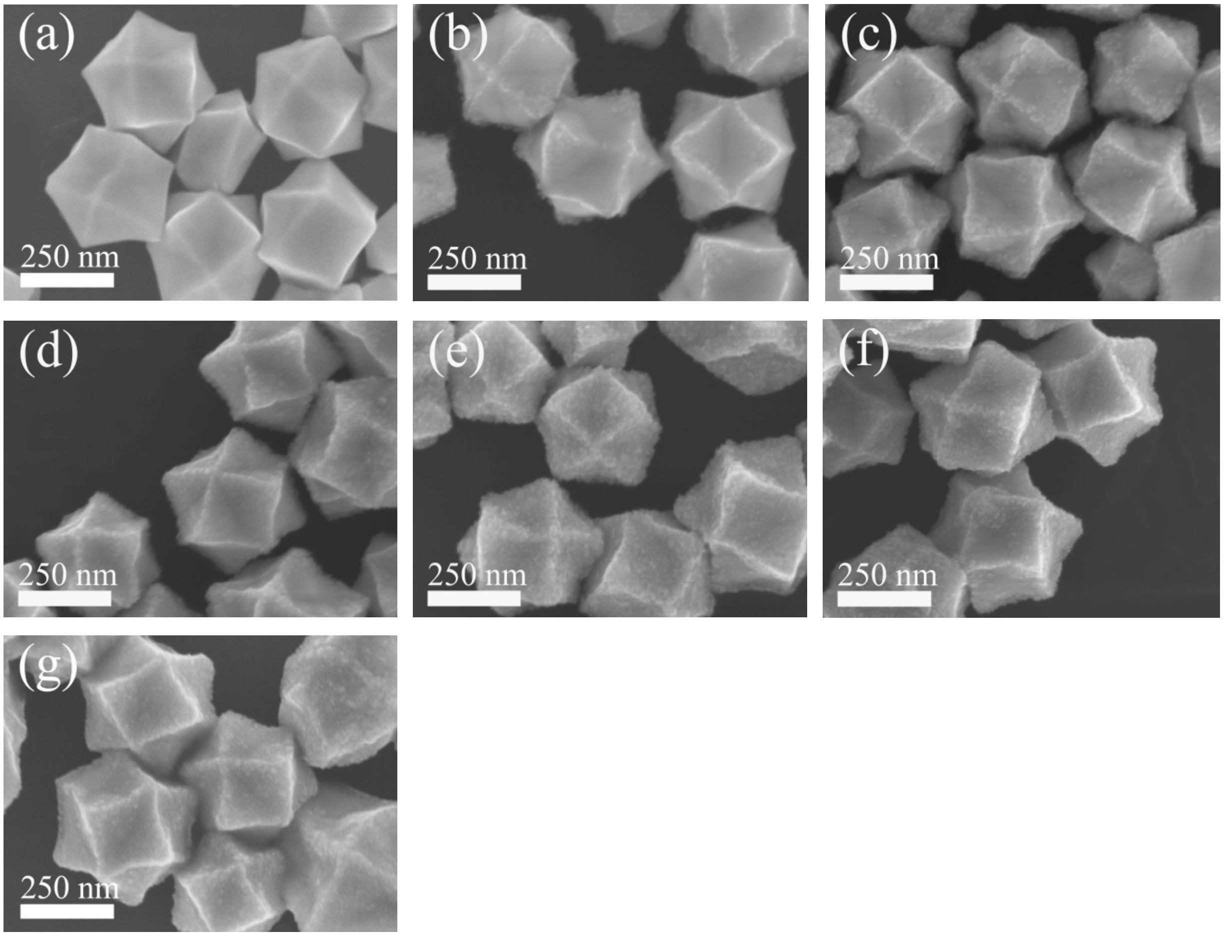

Figure S8. (a) SEM image of Au HNPs. (b)-(g) SEM images of 35-Au@AgPt NPs synthesized for different growth times 5, 10, 15, 25, 40 and 60 min, respectively.

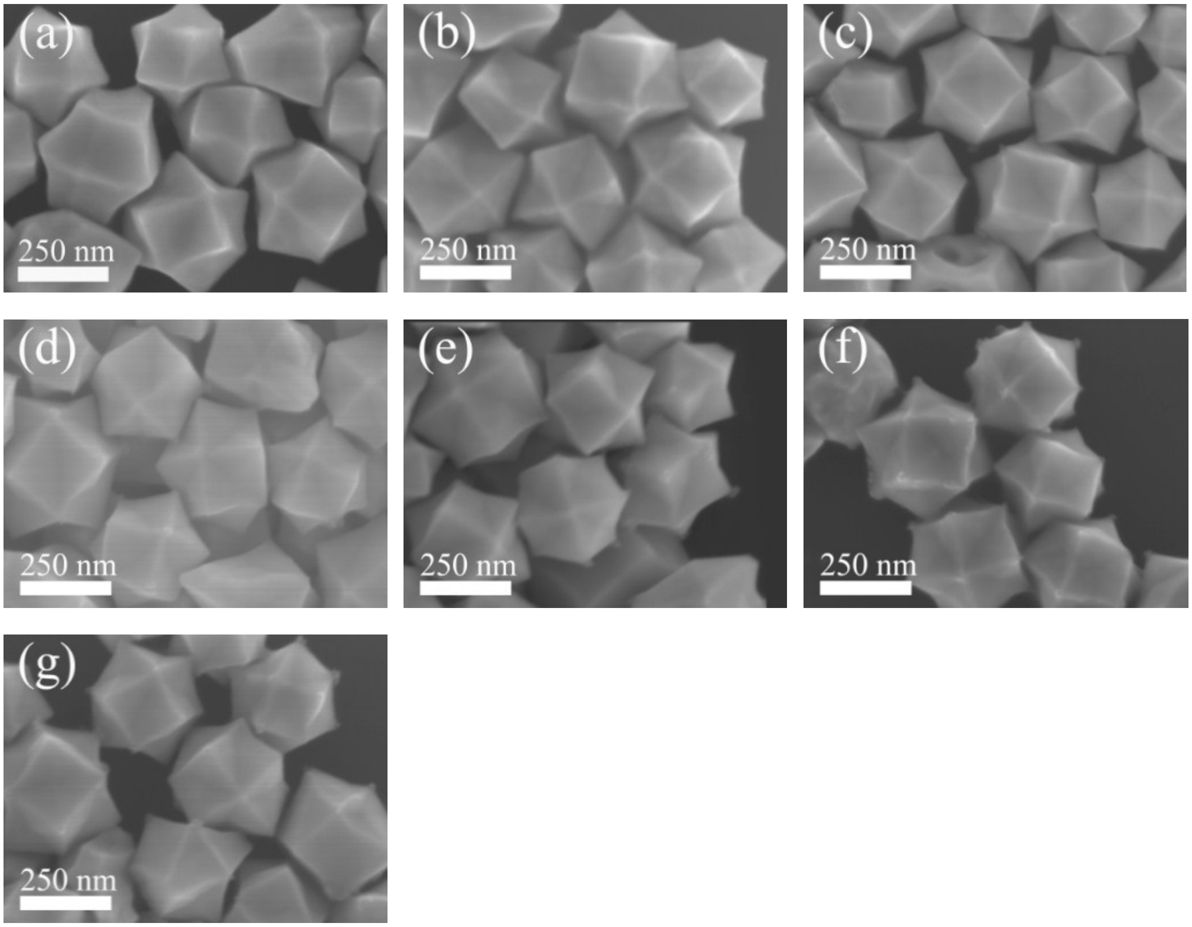

Figure S9. SEM images of 20-Au@AgPt NPs synthesized by different amounts of Pt precursor: (a) 5 μL, (b) 10 μL, (c) 15 μL, (d) 20 μL, (e) 25 μL, (f) 30 μL and (g) 60 μL.

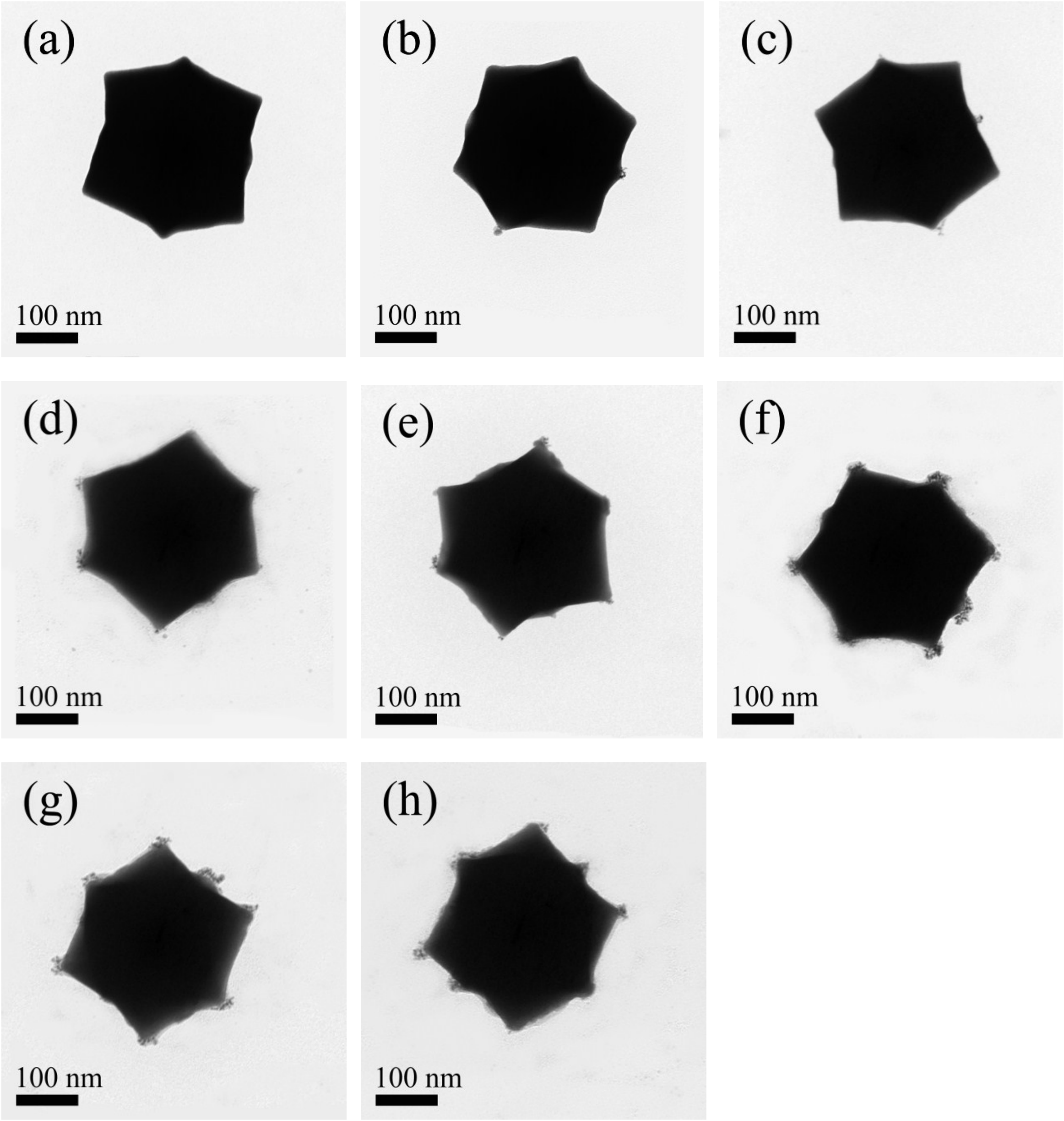

Figure S10. (a) TEM image of an individual Au HNP. TEM images of 20-Au@AgPt NPs synthesized by different amounts of Pt precursor: (b) 5 μL, (c) 10 μL, (d) 15 μL, (e) 20 μL, (f) 25 μL, (g) 30 μL and (h) 60 μL.

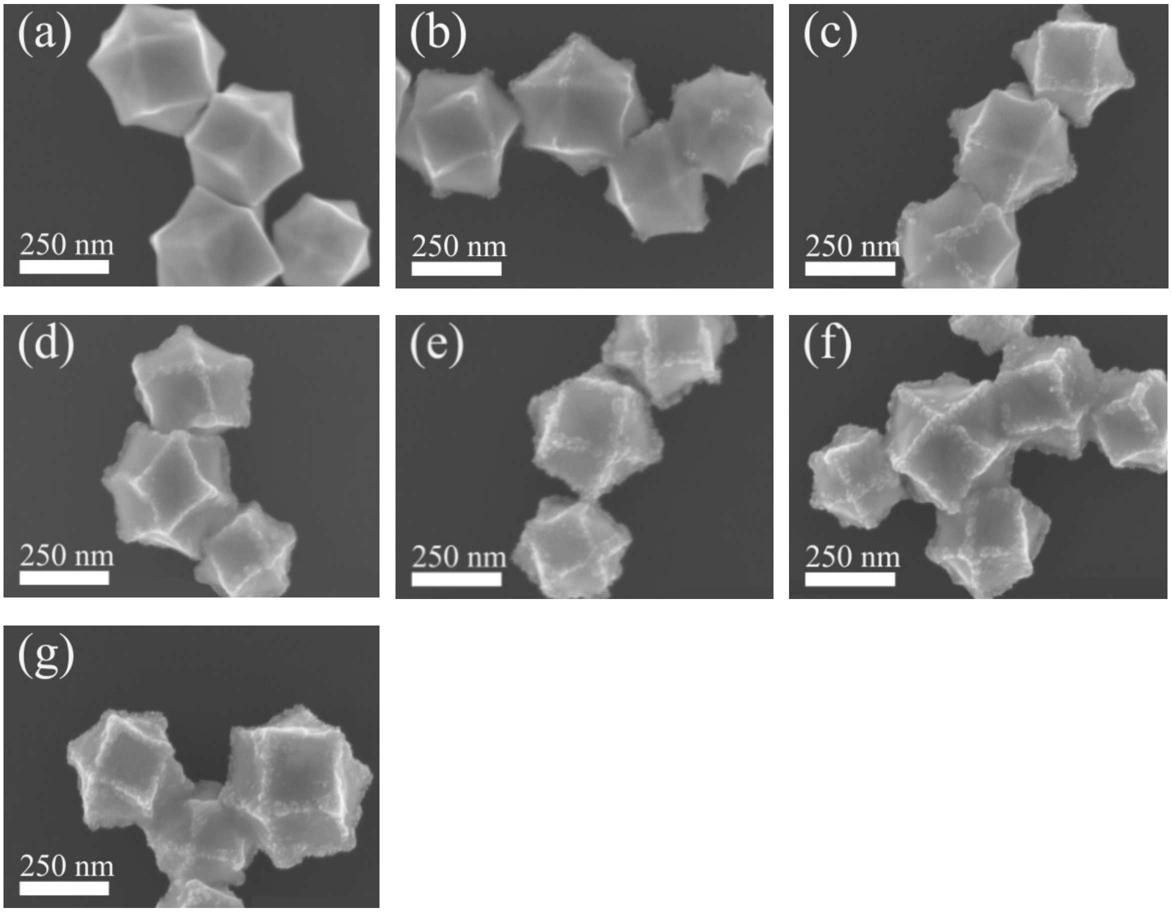

Figure S11. (a) SEM image of Au HNPs. SEM images of 25-Au@AgPt NPs synthesized by different amounts of Pt precursor: (b) 5 µL, (c) 10 µL, (d) 20 µL, (e) 30 µL, (f) 40 µL and (g) 60 µL.

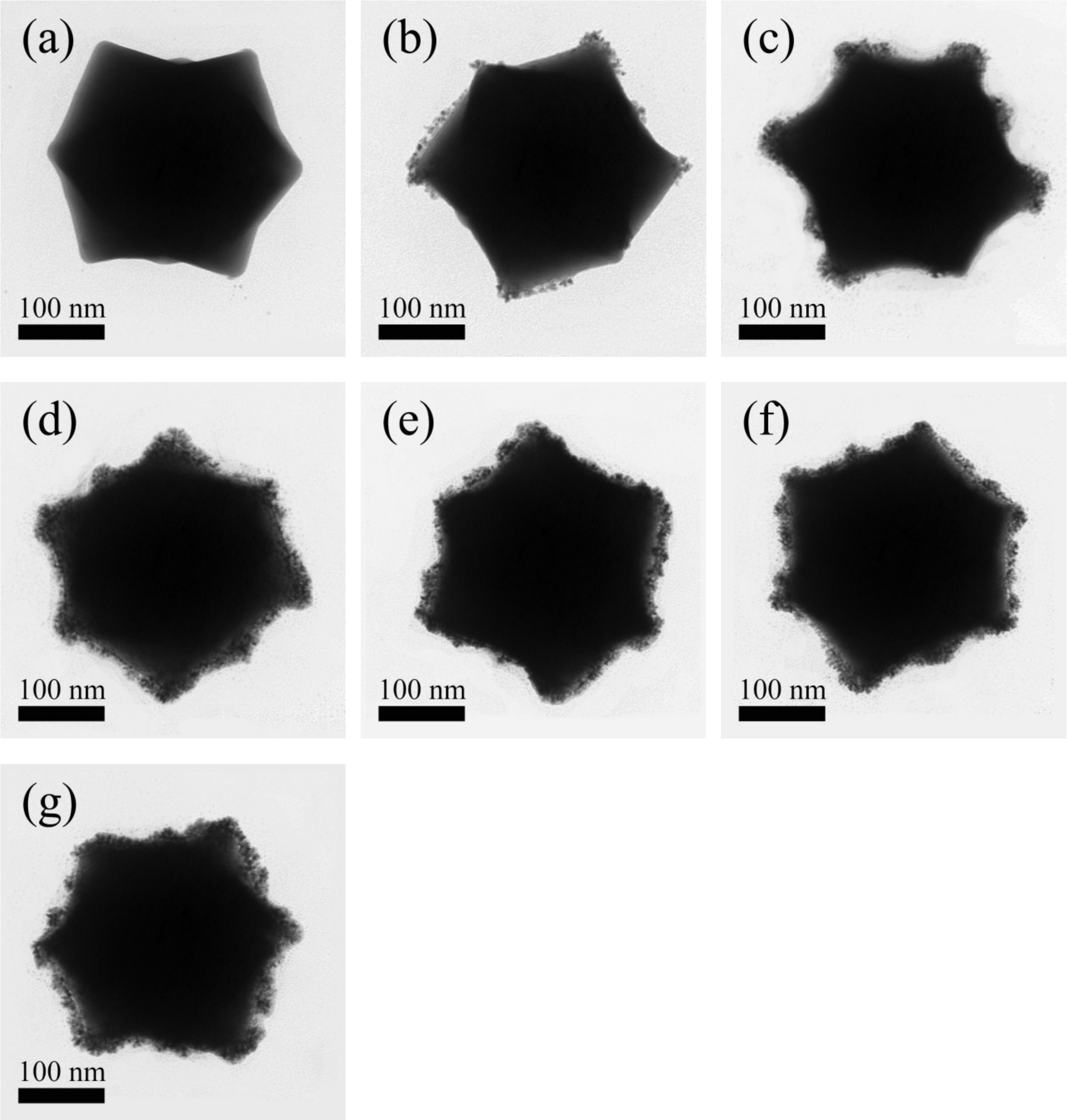

Figure S12. (a) TEM image of an individual Au HNP. TEM images of 25-Au@AgPt NPs synthesized by different amounts of Pt precursor: (b) 5 μL, (c) 10 μL, (d) 20 μL, (e) 30 μL, (f) 40 μL and (g) 60 μL.

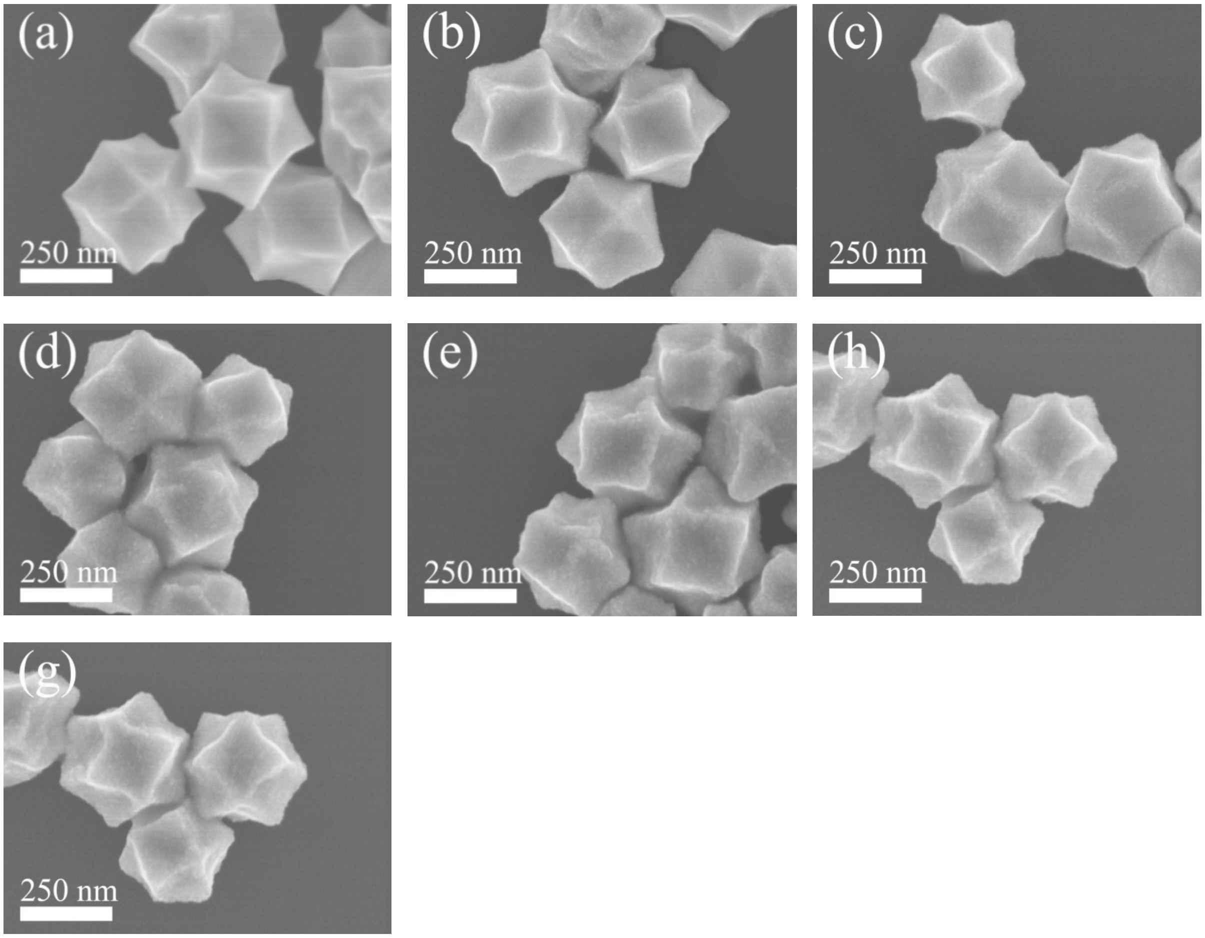

Figure S13. (a) SEM image of Au HNPs. SEM images of 35-Au@AgPt NPs synthesized by different amounts of Pt precursor: (b) 5 μL, (c) 10 μL, (d) 20 μL, (e) 40 μL, (f) 60 μL and (g) 80 μL.

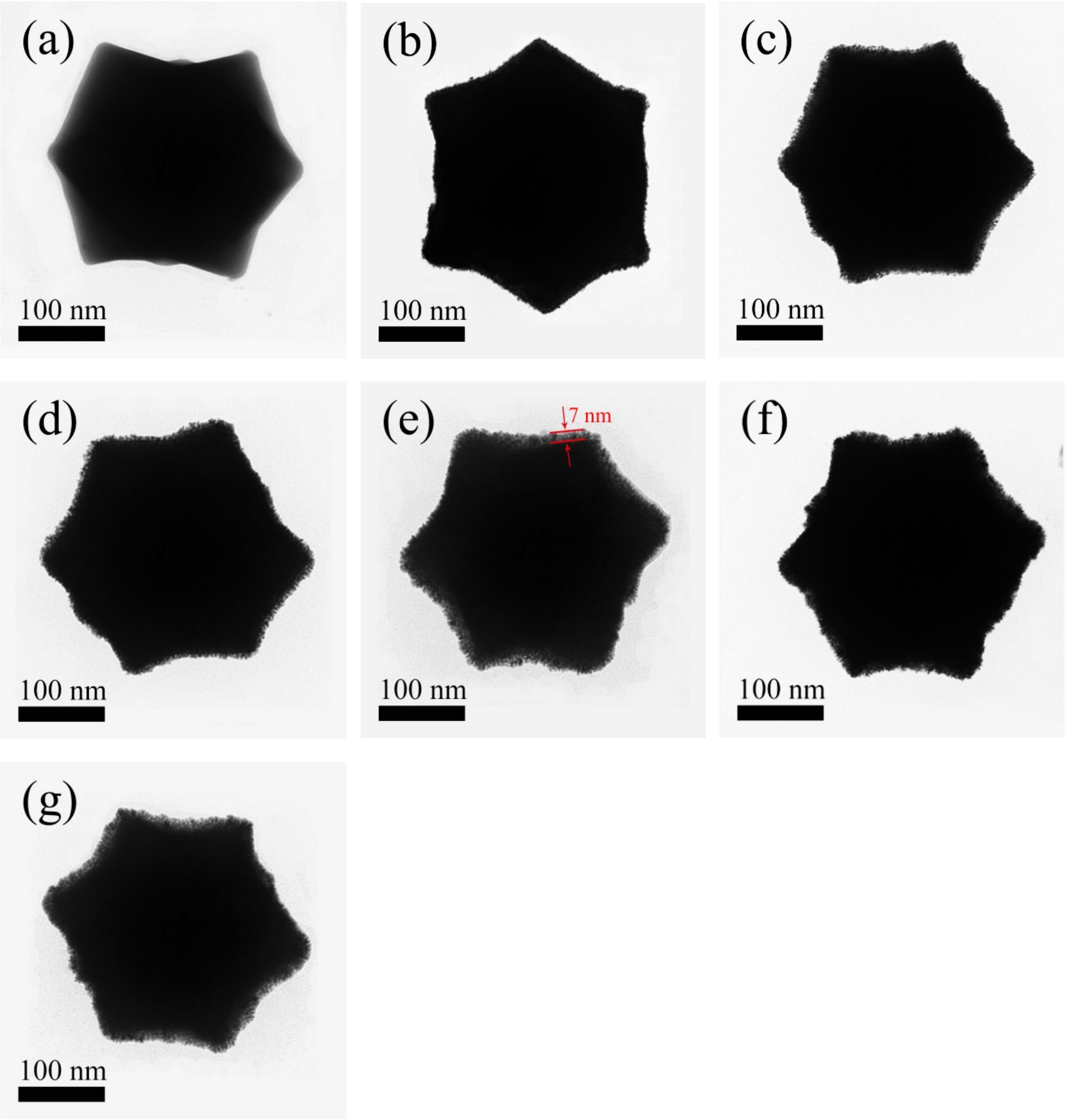

Figure S14. (a) TEM image of an individual Au HNP. TEM images of 35-Au@AgPt NPs synthesized by different amounts of Pt precursor: (b) 5 μL, (c) 10 μL, (d) 20 μL, (e) 40 μL, (f) 60 μL and (g) 80 μL.

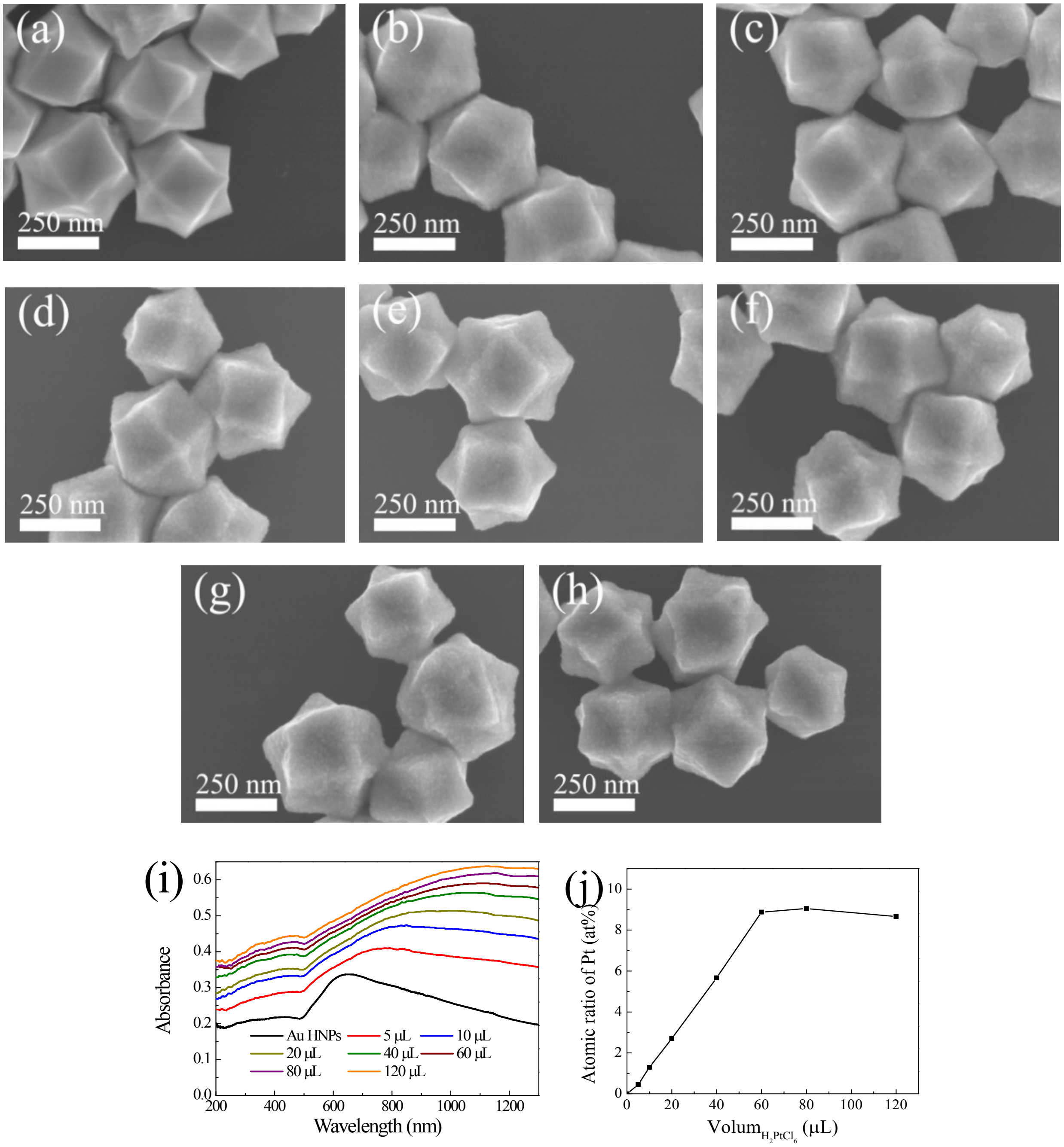

Figure S15. (a) SEM image of Au HNPs. SEM images of 50-Au@AgPt NPs synthesized by different amounts of Pt precursor: (b) 5 μL, (c) 10 μL, (d) 20 μL, (e) 40 μL, (f) 60 μL, (g) 80 μL and (h) 120 μL. Corresponding absorption spectra (i) and EDS data (j) of 50-Au@AgPt NPs synthesized by different amounts of Pt precursor.

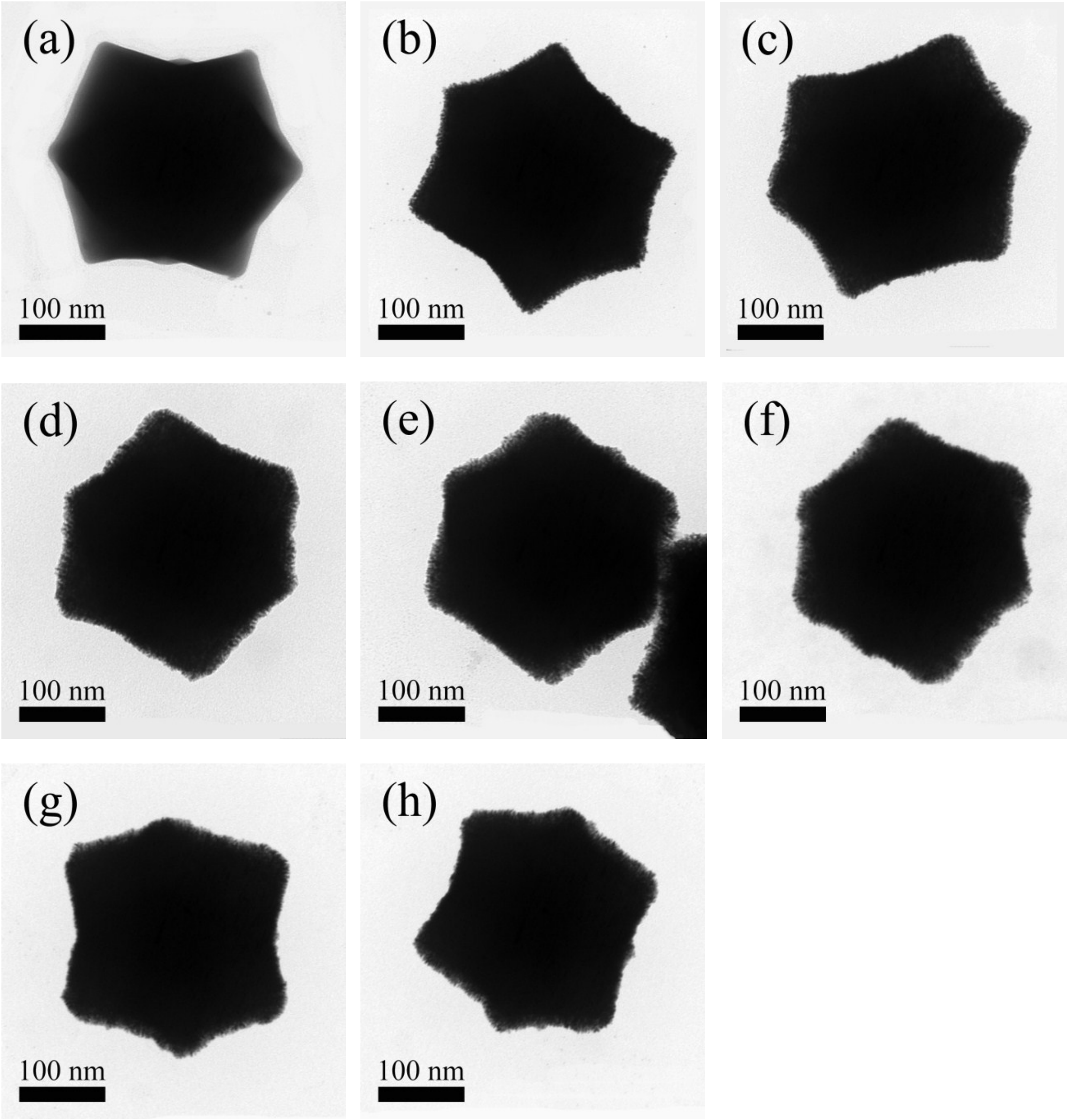

Figure S16. (a) TEM image of an individual Au HNP. TEM images of 50-Au@AgPt NPs synthesized by different amounts of Pt precursor: (b) 5 μL, (c) 10 μL, (d) 20 μL, (e) 40 μL, (f) 60 μL, (g) 80 μL and (h) 120 μL.

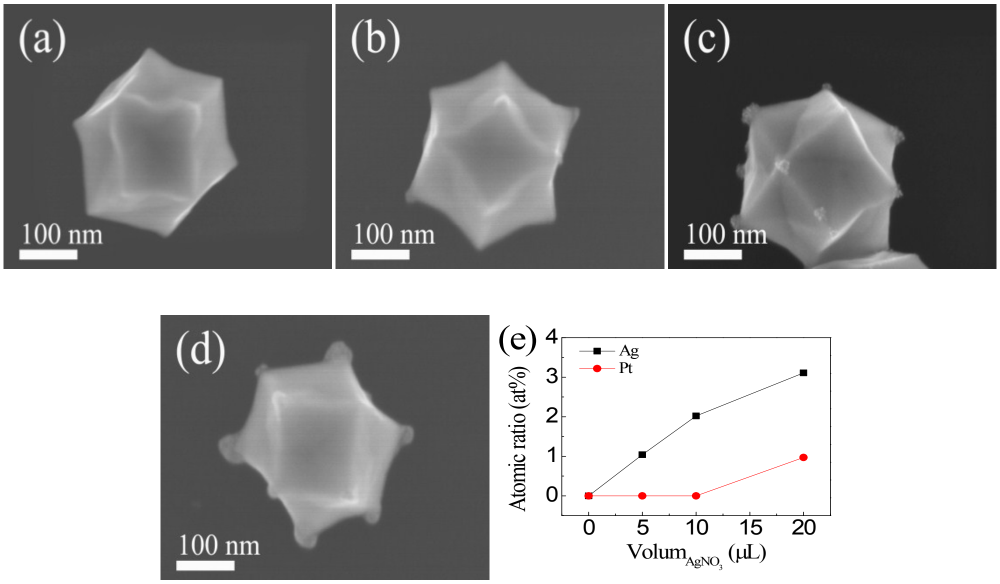

Figure S17. SEM images of 20-Au@AgPt NPs synthesized by different amounts of $AgNO_3$: (a) 0 μL, (b) 5 μL, (c) 10 μL and (d) 20 μL. (e) EDS data of 20-Au@AgPt NPs synthesized by different amounts of $AgNO_3$.

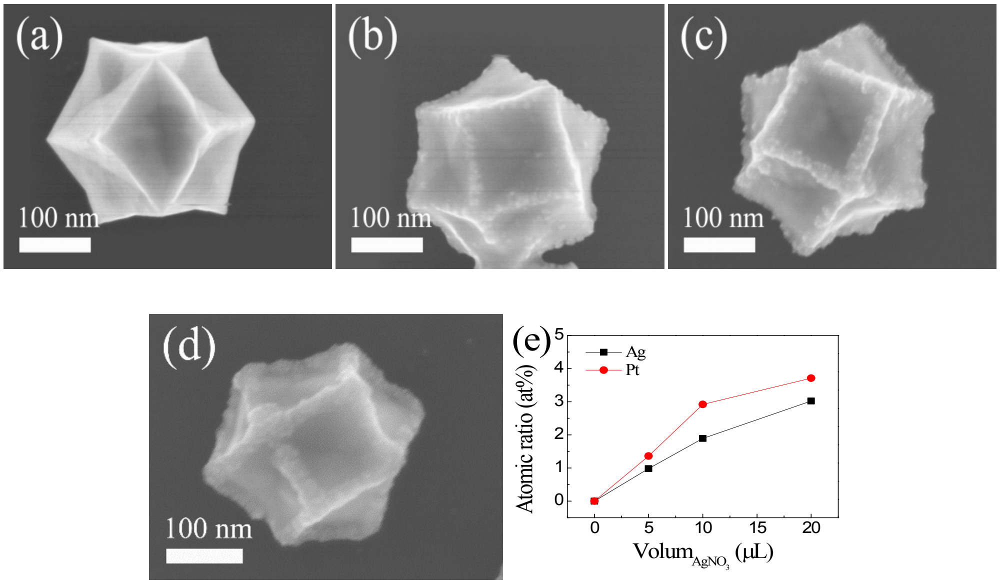

Figure S18. SEM images of 25-Au@AgPt NPs synthesized by different amounts of $AgNO_3$: (a) 0 μL, (b) 5 μL, (c) 10 μL and (d) 20 μL. (e) EDS data of 25-Au@AgPt NPs synthesized by different amounts of $AgNO_3$.

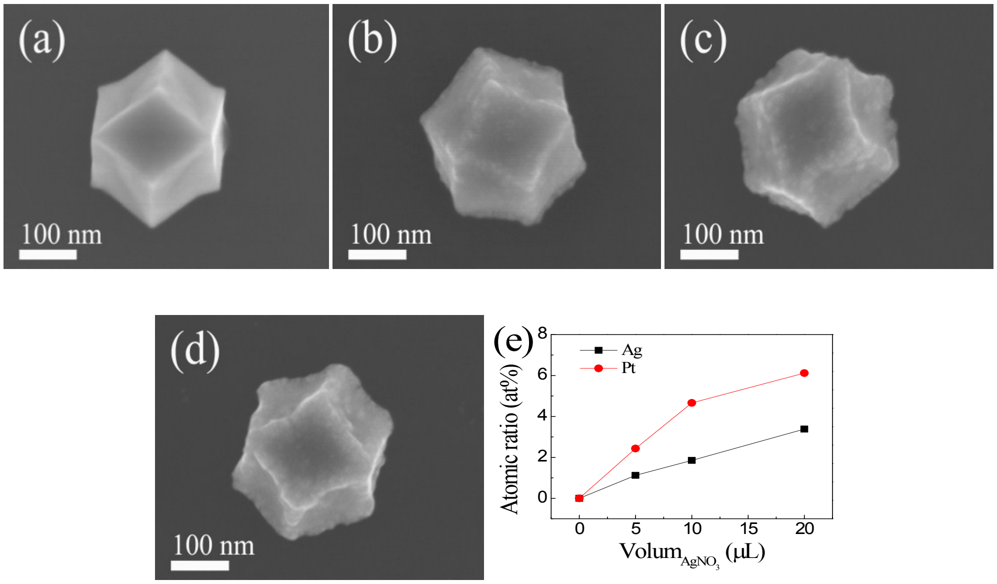

Figure S19. SEM images of 35-Au@AgPt NPs synthesized by different amounts of $AgNO_3$: (a) 0 μL, (b) 5 μL, (c) 10 μL and (d) 20 μL. (e) EDS data of 35-Au@AgPt NPs synthesized by different amounts of $AgNO_3$.

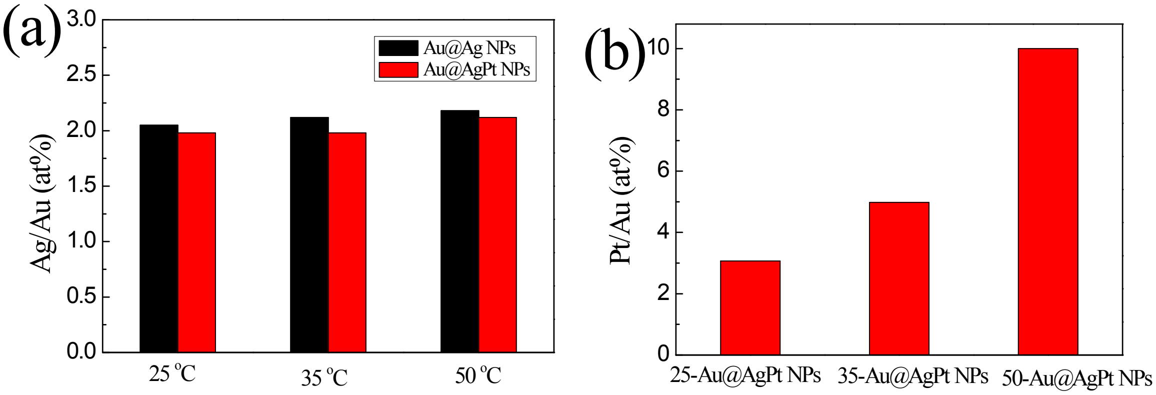

Figure S20. (a) The content of Ag element in the Au@Ag NPs before and after deposition of Pt at 25°C, 35°C, and 50°C. (b) The content of Pt element in the 25-Au@AgPt NPs, 35-Au@AgPt NPs, and 50-Au@AgPt NPs. All the contents of Ag and Pt were normalized, whereby each value was divided by the content of Au in the corresponding nanopartcicles.

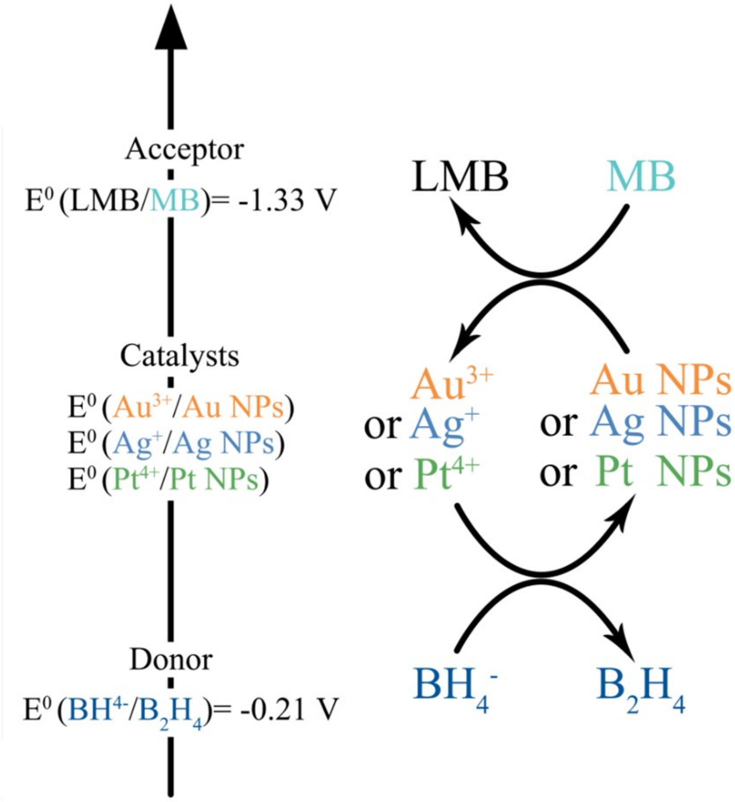

Figure S21. Schematic illustration of the catalytic reaction between MB and $NaBH_4$ with the Au@AgPt NPs as catalysts. The mechanism of catalytic electron transfer where the metal nanoparticles relay the electron from the donor to the acceptor. LMB: leuco methylene blue.

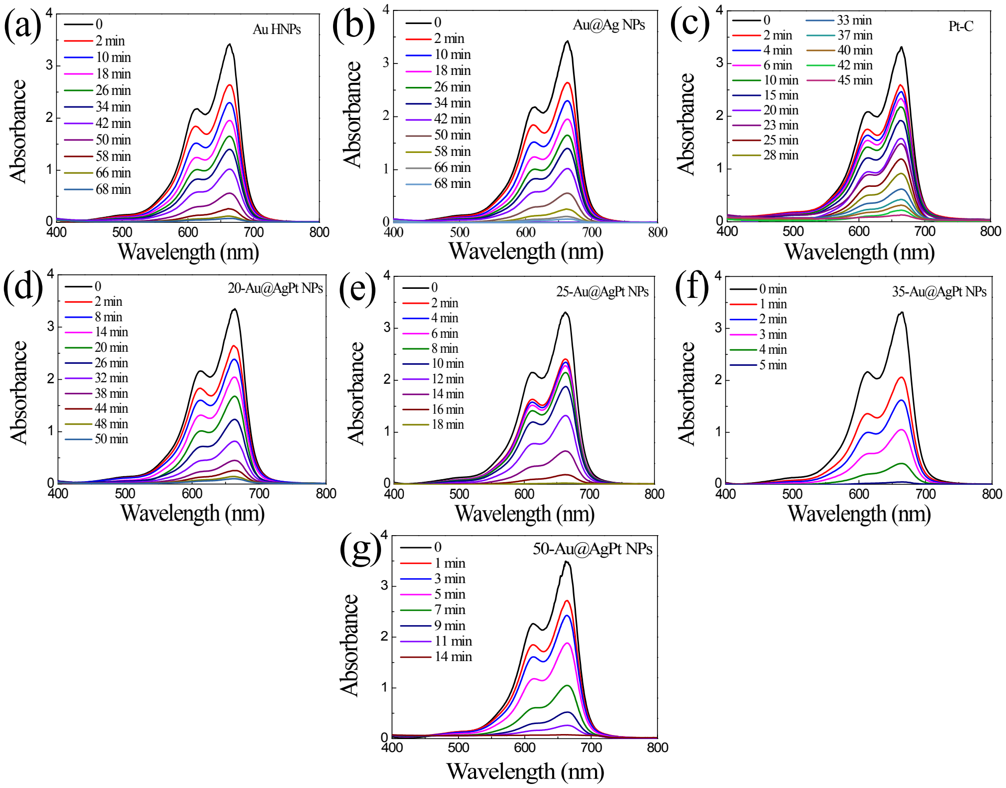

Figure S22. Time-dependent absorption spectra of MB reduced by NaBH$_4$ in the presence of (a) Au HNPs, (b) Au@Ag NPs, (c) Pt-C, (d) 20-Au@AgPt NPs, (e) 25-Au@AgPt NPs, (f) 35-Au@AgPt NPs and (g) 50-Au@AgPt NPs.

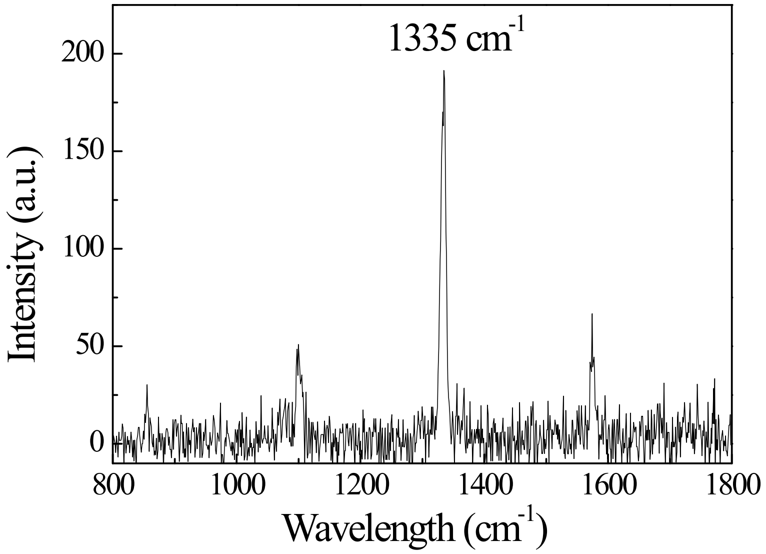

Figure S23. Normal Raman spectrum of 4-NTP.

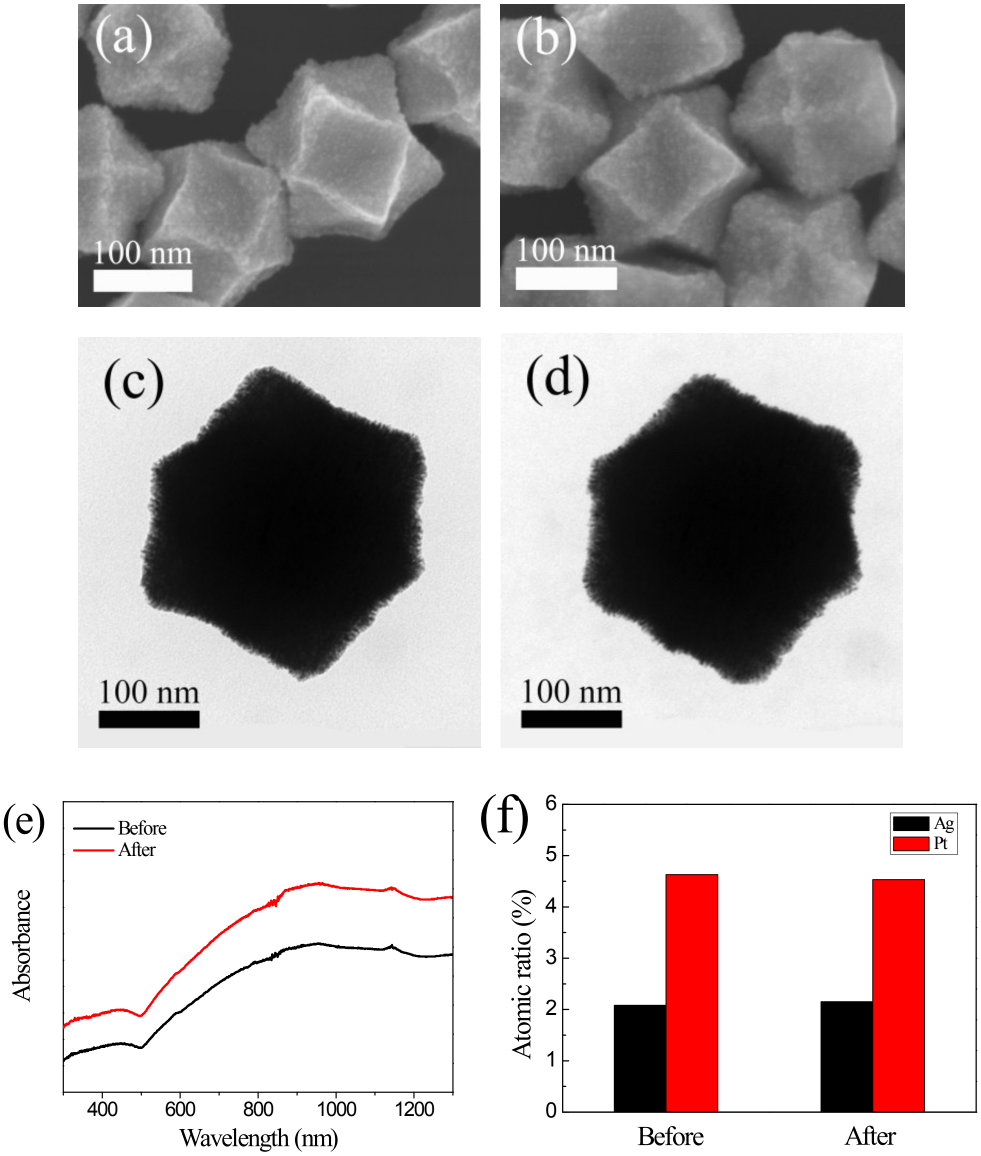

Figure S24. Characterizations of the 35-Au@AgPt HNPs before and after catalytic and SERS performances. SEM images: (a) before and (b) after. TEM images: (c) before and (d) after. (e) Absorption spectra. (f) Element contents.